Systematic errors in GAIA's radial velocity measurements: II. Extension to other spectral types.

M. David, Astrophysics research group, University of Antwerp
RVS-MD-002

February 6, 2002

1 Introduction.

In the present contribution we amend two shortcomings of the previous one (RVS-MD-001), notably the fact that the wavelength range did not comply with the constraints set in RVS-CoCo-001, and the fact that only the solar spectrum was used. Also an error in the simulation software has been corrected. We refer to RVS-MD-001 for the definition of all concepts and notations to be used here, as well as for the experimental set-up.

In Sect. 2 we make two points about terminology. The amended results for the solar spectrum are shown in Sect. 3. In Sect. 4 we discuss the results of simulations with the synthetic spectra produced by the Padova-Asiago group; the need to find suitable continuum windows near the ends of the wavelength range for a wide variety of spectra, has drawn attention the fact that the present wavelength limits (8490Å,8740Å) are often unfortunate for RV measurements, if they are to be taken literally, so we suggest a small extension.

2 Notes on terminology.

One of the errors discussed in RVS-MD-001 was the so-called *discretization error*. It is caused by the fact that the cross-correlation (CC) function is known only in sampled form, that we have to interpolate its values in order to estimate the sub-pixel position of the CC-maximum and that this interpolation cannot be exact since we cannot use the true shape of the CC-function to effect it. In an earlier report (Katz et al. 1999), however, this error was referred to as *sampling error* and since the latter term seems altogether a better one, henceforth I shall use that instead of the former.

The second point is more important. It concerns the term *accuracy* which, in the past reports on GAIA instruments, has been used frequently in connection with the magnitude of random errors. I would like to draw attention to the fact that this is not a correct usage of this term. In textbooks on the analysis of experimental data (e.g. Cochran & Cox, 1957) it is clearly stated that *precision* describes the repeatability of a (possibly erroneous) measurement, i.e. the magnitude of random errors, whereas *accuracy* describes the proximity of a measured value (or of a set of these) to the true value, i.e. the magnitude of systematic errors or bias. At least among the people concerned with radial velocities (but probably also in the wider astronomical community) several authors in the past have reminded their readers of the distinction between those terms (e.g. Latham 1978, Dravins 1994, Griffin 1999). Especially in situations where one has to deal with both random errors and systematic errors, it is really helpful to adhere to the correct usage and I would therefore urge all colleagues in the GAIA community to do likewise.

3 Corrected results for the solar spectrum.

The simulations reported in RVS-MD-001 were done using wavelength intervals which do not comply with the agreed GAIA range (8490 Å$\leq \lambda \leq$8740 Å); moreover I noted afterwards that, owing to the way the cross-correlation function is calculated in MIDAS, the intervals which were used effectively in these simulations had lost some 10 Å at each end in comparison with the ones I described. Therefore (and after correcting the latter flaw) I repeated the simulations with the wavelength intervals [8494,8702], [8494,8723] and [8494,8732].

The reason for taking 8494Å as the lower bound rather than 8490Å is that the cross-correlation requires the availability of a few extra pixels beyond the chosen boundaries. Again the choice of the different redward boundaries was made so as to enable an estimate of the boundary effect from a comparison of the results obtained with each of them, i.e. one is a "careful" choice while the other two are somewhat less appropriate in the sense that they are located in a continuum-window which is too narrow to avoid boundary effects when there is considerable rotational broadening (at $v_{\rm rot} > 50\,{\rm km\,s^{-1}}$ the wings of adjacent lines spill over these boundaries and affect the shape (and thus also the centroid) of the cross-correlation peak).

The results are shown in Figs. 1 and 2. As expected, one can see that the behaviour of the displayed data is qualitatively the same as with the old wavelength intervals; in particular the error caused by a difference in the deformation of spectral lines by star-line curvature (SLC) in Fig. 2b is virtually identical to Fig. 4 of RVS-MD-001. However, quantitatively there are two differences which require some comment. Firstly, in Fig. 1a the monotonous decrease of the sampling error with increasing rotational broadening occurs only for $v_{\rm rot} \leq 50{\rm km\,s^{-1}}$; this appears to be due to the wing of the CaII 8498Å line extending across the boundary at higher $v_{\rm rot}$ and so causing the CC peak to deviate more from the gaussian shape; this can be avoided by shifting the blueward boundary down to 8490Å (Fig. 1b) but then within the present GAIA constraints the four extra pixels required for the cross-correlation would not be available.

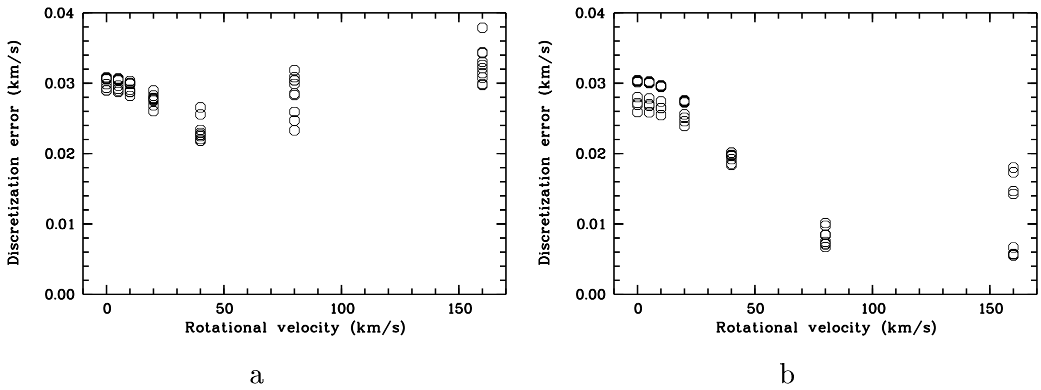

Figure 1: The sampling error as a function of rotational broadening, obtained with the blueward boundary at (a) 8494Å and (b) 8490Å respectively.

Secondly, the magnitude of the boundary error is much less than what we found in RVS-MD-001 ; this is due to the particular choice of the "optimal" boundary point (i.e. the one in a truly broad continuum window) at 8632Å in the earlier simulations: the corresponding wavelength interval did *not* include the strong CaII line at 8662Å while the other intervals did, and owing to the variation of the star-line curvature with varying wavelength, the absence, resp. presence of this strong line caused the SLC-mismatch error to differ considerably between the "optimal" interval and the other two; since the boundary error is estimated as the maximal difference between the *total* errors obtained with different boundaries, it was thus contaminated badly by the SLC-mismatch. Although it is good news that the rather

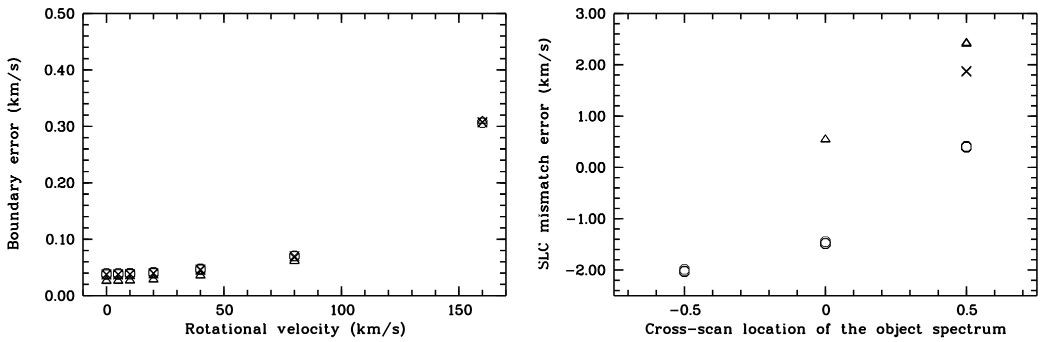

a b

Figure 2: (a) the boundary error as a function of rotational broadening; (b) the error due to a difference in the effect of star-line curvature on two spectra of the same object.

high values we found earlier were an over-estimate, we shall see further on that, for stars of higher temperature and higher metallicity, high values of the boundary error do reappear.

4 Other spectral types.

4.1 The input data.

The Padova-Asiago group has produced a library of synthetic spectra which was distributed on CD-rom during the GAIA-meeting at ESTEC on June 25 2001. A part of this library was used in an automated repetition of the simulations previously done for the solar spectrum. Our sub-grid comprises the metallicities [Fe/H] = -2,-1,0,+0.5, the surface gravities $\log g = 1, 2, 3, 4$, the temperatures $T_{\rm eff}$ = 4750,5750,6250,6500,7250,9750,30000°K and the rotational velocities $v_{\rm rot}$ = 0,10,20,50,100,200,400 $\rm km\,s^{-1}$. Not all possible combinations of these parameters were available in the library (nor, indeed, meaningful: one does not expect to encounter fast-rotating late-type stars in practice) and it is regrettable that only two early-type sets were produced, but for the present purpose the resulting sample of 600 spectra is probably sufficiently representative of what we can expect to encounter in the GAIA observations.

The spectra were rebinned to equal steps in $\ln(\lambda)$ of $0.88\,10^{-4}$ which corresponds to 0.75Å at $\lambda = 8520$ Å. Since a more realistic model for the PSF was not yet available at the time these calculations were begun, this rebinning was done with the same model for the effective PSF as before, i.e. a gaussian in $\ln(\lambda)$ with $\sigma = 1$ px, deformed by the star-line curvature.

4.2 Remarks about the experimental procedure.

As we did with the solar spectrum, each object in the sample was rebinned with a gaussian PSF and with the (asymmetrical) "effective PSF" (EPSF) corresponding to three different locations in the FOV; each of these results was furthermore reproduced eightfold, each time shifted over $1/8^{\rm th}$ of a pixel. We cross-correlated the spectrum resulting from each EPSF with itself and and with each of its shifted versions, as well as with the spectra resulting from the other EPSF's and with their shifted versions to estimate both the sampling error and the SLC-mismatch error; the same cross-correlations were done over three slightly different wavelength intervals to estimate the boundary error.

The choice of the boundaries for the cross-correlation intervals was made as follows. It would have been impracticable to consider each spectrum in the sample individually, so it was inevitable that the choice would be less than optimal for many cases. Visual inspection showed that, at least if $v_{\rm rot} = 0$, a choice made at a given temperature for the spectrum with the highest surface gravity and the highest metallicity would be equally good or better for all other spectra of the same $T_{\rm eff}$. The intervals $[\lambda_0, \lambda_i]$, i=1,2,3 thus adopted for each temperature (within the GAIA limits and so that the boundaries lie in an acceptable continuum window at least if $v_{\rm rot} = 0$) are given in Table 1. The selection in this table necessitates

Table 1: Cross-correlation intervals.

$T_{\rm eff}$ (°K)	λ_0 (Å)	λ_1 (Å)	λ_2 (Å)	λ_3 (Å)
4750	8523.0	8695.0	8707.0	8722.0
5750	8523.0	8707.0	8722.0	8732.0
6250	8521.5	8707.0	8722.0	8732.0
6500	8521.5	8707.0	8722.0	8732.0
7250	8521.5	8707.0	8715.3	8722.0
9750	8494.0	8699.0	8707.5	8715.0
30000	8494.0	8702.0	8715.0	8722.0

the following comments. First of all, it is obvious that choosing the blueward boundary at 8523.0 Å or at 8521.5 Å is undesirable because it means we jettison the CaII line at 8498 Å and Paschen 16. Yet, in particular for $T_{\rm eff} = 6250, 6500, 7250$ it cannot be avoided since at the farthest blueward point which could be considered as a boundary within the GAIA limits (notably 8494 Å) the slope of the CaII line is still far too strong. If one wishes to include the region around 8498 Å the boundary had better be chosen at 8486.5 Å. Similarly, although less dramatic, there are cases where it is obvious that the redward boundary would be much better at 8745 Å than at 8732 Å. Although the present GAIA limits are the result of careful consideration and are undoubtedly very adequate for many purposes, we thus find that, from the point of view of RV measurements using cross-correlation, some additional opportunities for selecting appropriate continuum windows near the ends of the range, could help a great deal to optimize the RV measurement. Actually an extension of a mere 10 Å at both ends would be fine.

Furthermore, from visual inspection one finds that, at higher rotational velocities ($> 100\,{\rm km\,s^{-1}}$), some of the redward boundaries become truly inappropriate and in some cases it would not even be possible to find a replacement for all of them. Therefore I did not attempt to adapt the selection in Table 1 to rotational broadening and merely checked that the (inevitably increased) boundary effects at higer $v_{\rm rot}$ do not affect the SLC-mismatch error which is still our main concern.

Finally one also sees that, at $T_{\rm eff} > 6000$, the blueward end of the spectrum is no longer close to the continuum level anyway because the wings of the CaII lines and of the Paschen lines all begin to overlap. In practice this fact may become hidden if some rectification is applied to the spectra. However, apart from the question whether it is desirable to thus replace the true continuum by a speudo-continuum (in which process the spectral lines might be deformed) such a rectification would require an almost individual treatment of all the spectra in the sample, which was impracticable at this stage. So I simply ignored the fact that the intensity in the vicinity of the blueward boundary is sometimes at only 90% or even 80% of the continuum level. As a consequence in those cases CC peak acquired a sloping "background" which not only biased the peak-position measurement but also caused the CC peak to become so asymmetric (especially at higher $v_{\rm rot}$) that it was no longer possible to use a gaussian as the interpolating function (or "fit-model") in the actual centroiding procedure. Therefore, instead of a gaussian a $4^{\rm th}$-degree polynomial was used for all spectra. Although this causes the sampling error to be comparatively much larger for sharp-lined spectra[1] it

[1]In fact the sampling error depends very much on the model which is used for the peak in the centroiding procedure, and was therefore originally also termed *model-mismatch error* (David & Verschueren 1995); at

undoubtedly provides a much more robust centroiding.

4.3 Results.

The main reason for considering a wide range of spectral types is to find out if there is any important correlation between the magnitude of systematic errors and the atmospheric parameters. As it happens the results for the sampling error and for the boundary error on the whole do not provide a clear-cut answer to this question. Although for each individual object in our sample the behaviour of both of these quantities as a function of $v_{\rm rot}$ appears to be qualitatively similar to their behaviour for the solar spectrum, their actual magnitude varies rather strongly with each of the atmospheric parameters; plotting them against $T_{\rm eff}$, $\log g$ or [Fe/H] yields graphs which are characterized by a large scatter which increases with increasing $T_{\rm eff}$ and $\log g$ but is roughly independent of the metallicity. A more detailed study might yet reveal additional detail but in view of the preliminary character of the present work (owing to the facts that the PSF is still only a naive model, the pixel-size and the wavelength-constraints may yet change, there is no decision yet as to how spectra with a sloping pseudo-continuum will be handled, etc.) such an effort seems unwarranted at present.

In order to to illustrate crudely how the errors depend on the atmospheric parameters, in the figures below we distinguish two temperature groups (in separate frames), two gravity groups and two metallicity groups (by different symbols).

The most striking difference between the two temperature groups in Fig. 3 is in the scale of the sampling errors. The large values found for the higher temperatures must be ascribed to a contamination by the slope in the pseudo-continuum which deforms the CC peak and so falsifies the rather delicate sub-pixel-position measurements. This deformation is further aggravated by the effect of very strong rotational broadening. The fact that in the lower temperature group the errors are still an order of magnitude larger than in Fig. 1 is due to the use of a $4^{\rm th}$-degree polynomial instead of a gaussian as a fit-model for the CC peak, as explained above; it is to be noted, though, that a gaussian leads to completely nonsensical results for many of the high-temperature objects. The value of the metallicity does not seem to make much difference, but the surface gravity does, at least in the higher temperature group: objects with higher $\log g$ clearly produce larger sampling errors, which again must be ascribed to the contamination of position measurements by the slope of the pseudo-continuum.

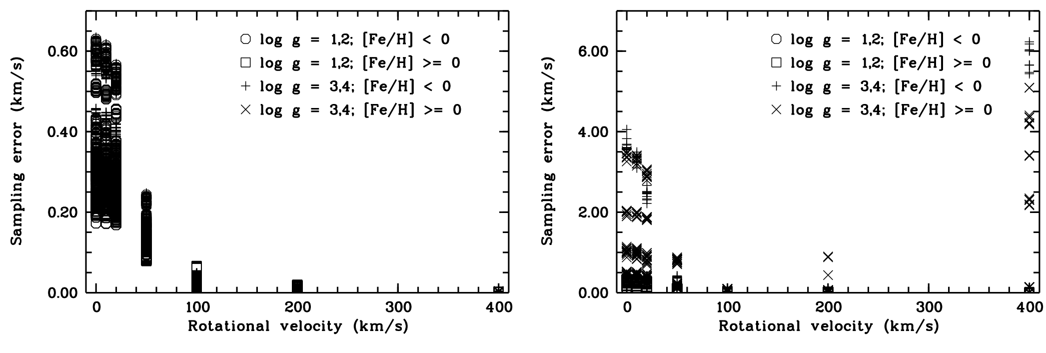

a b

Figure 3: The sampling error as a function of rotational broadening for all objects with (a) $T_{\rm eff} < 7000°$K and (b) $T_{\rm eff} > 7000°$K.

the lowest $v_{\rm rot}$ a $4^{\rm th}$-degree polynomial is unable to model the sharp CC peak properly, hence the increased sampling error, but as the rotational broadening increases, on the contrary, the weakening curvature of the CC peak renders the fit af a gaussian increasingly unstable (its position becoming particularly sensitive to any asymmetry in the data) while the polynomial becomes amply sufficient to the represent the shape of the peak; this explains the fact that the general decrease of the sampling error towards higher $v_{\rm rot}$ in Fig.3a below, is considerably stronger than the decrease observed in e.g. Fig. 1b.

The graphs of the boundary error (Fig. 4) in the first place show the expected strong increase with increasing rotational broadening. Undoubtedly the very highest values occurring here could have been reduced somewhat by shifting the boundaries according to the local pseudo-continuum, but the general trend would remain the same. In the higher-temperature group, although the metal lines are much weaker, the effect of rotation is aggravated by the strengthening of the Paschen lines. Again the metallicity does not appear to make a great deal of difference but of course increasing gravity does, through the increased Stark-broadening of the Paschen lines.

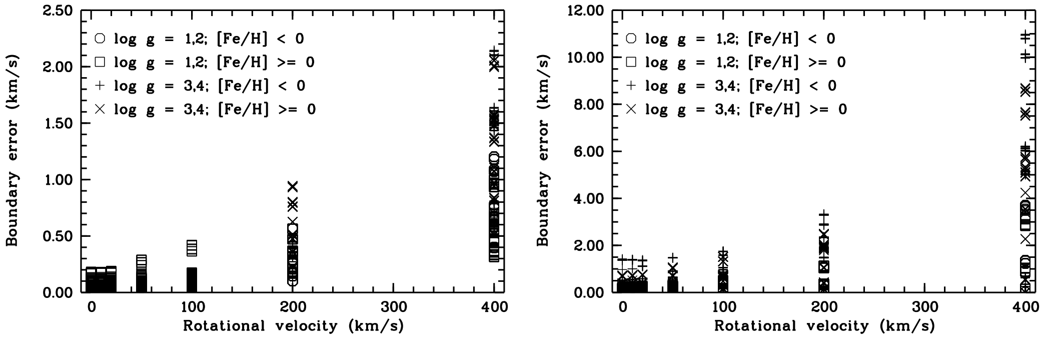

a b

Figure 4: The boundary error as a function of rotational broadening for all objects with (a) $T_{\rm eff} < 7000°$K and (b) $T_{\rm eff} > 7000°$K.

The SLC-mismatch error, at least, does offer a reasonably clear picture: although its values are spread out somewhat around those obtained for the sun, the dispersion is quite modest even in the high-temperature group. The larger dispersion we find in the high-temperature group for the objects at FOV-position 0.5 (and which, incidentally, appears to come in particular from objects with $T_{\rm eff} = 9750°$K and $v_{\rm rot} \leq 100\,{\rm km\,s^{-1}}$ and from objects with $T_{\rm eff} = 30000°$K and $v_{\rm rot} \geq 200\,{\rm km\,s^{-1}}$) will be studied in more detail later on, to find out whether it might be due to interference with some other source of deformation of the CC-peak. Anyway, since our fairly wide range of values for the atmospheric parameters turns out to lead to error values which are spread out so little, we may confirm our earlier tentative conclusion that the SLC-mismatch error depends only very weakly on the spectral structure. Judging from Fig. 5 it would therefore seem feasible in practice to reduce the effect of star-line curvature on RV measurements to a level of $0.5\,{\rm km\,s^{-1}}$, by means of a correction which depends only on the FOV-positions of template and object.

5 Conclusions.

- We found that the choice of a fit-model for the CC peak may seriously affect the sampling error; in practice this choice should therefore be considered carefully, in accordance with the accuracy requirements of the measurement and with the shape of the CC peak. For objects with higher $T_{\rm eff}$ and higher surface gravity we find sampling errors which are unacceptably large. In individual cases these could probably be avoided by a more careful choice of the boundary points and by rectifying the spectra prior to cross-correlation. However, apart from the fact that this might require some manual intervention for each object and so might not be feasible in practice, the rectification to an un-physical pseudo-continuum might itself introduce a systematic error in the RV measurement.

- The values of boundary error error given in RVS-MD-001 on the basis of the solar spectrum, were seriously over-estimated; nevertheless we now find that with other spectral

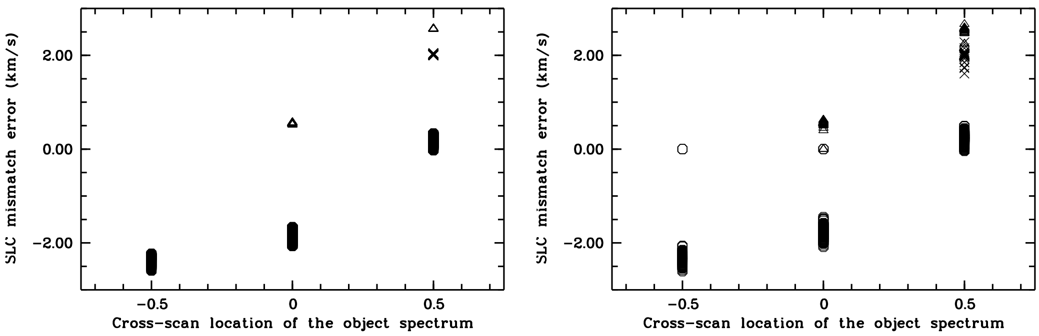

a b

Figure 5: The error due to a difference in the effect of star-line curvature on two spectra of the same object, for all objects with (a) $T_{\rm eff} < 7000°$K and (b) $T_{\rm eff} > 7000°$K. For each object the error is plotted as a function of the position of the object in the FOV, and the symbols distinguish different possibilities for the template: circles: template obtained with symmetrical EPSF; triangles: template from position -0.5; Crosses: template from position 0.0.

types, even higher values can in fact occur, even though the most extreme values in Fig. 4 must again be over-estimates caused by the absolute unsuitability of one or two of the three redward boundaries used to estimate the boundary error.

- For many spectral types, the limits of the wavelength range established at present for the RVS, are a little too tight to allow an optimal choice of the cross-correlation interval for RV measurements; an extension with e.g. 10 Å, especially at the blueward end, would help a lot.

- The effect of the star-line curvature on a RV measurement, which may amount to a bias of almost $3\,{\rm km\,s^{-1}}$, was found to be almost independent of the spectral structure; as a consequence, a correction depending only on the positions of the template and object spectra in the FOV, could reduce the bias to $0.5\,{\rm km\,s^{-1}}$ or less. if necessary, a further reduction based on dedicated simulations would also be feasible.

References

[1] Cochran, W.G., and Cox, G.M., 1957, Experimental Design, John Wiley & Sons Inc., New York.

[2] David, M., Verschueren, W., 1995, A&AS 111, 183-193.

[3] Dravins, D., 1994, The Impact of Long-Term Monitoring on Variable Star Research, Sterken, C. & de Groot, M. (eds), Nato science Series C,v. 436.

[4] Griffin, R.E.M., 1999, Precise Stellar Radial Velocities, Hearnshaw, J.B. & Scarfe, C.D. (eds.), ASP Conf. Ser. 185, 52.

[5] Latham, D.W.,1978, Modern Techniques in Astronomical Photography, West, R.M. & Hendier, J.L. (eds.), ESO Conference Proceedings, 141.